A Second-Order Time-Accurate Finite Element Method for Unsteady Incompressible Flow Analysis

Atipong Malatip[1], Niphon Wansophark[2] and Pramote Dechaumphai[3]

[1,2,3] Department of Mechanical Engineering, Faculty of Engineering, Chulalongkorn University,
Patumwan, Bangkok, 10330, Thailand,
Tel: 0-2218-6621, Fax: 0-2218-6621 [3]E-mail: fmepdc@eng.chula.ac.th

Abstract

A fractional four-step finite element method for solving unsteady incompressible fluid flow and heat transfer problems is presented. The second-order fully implicit Crank-Nicolson scheme is used for time integration and the resulting nonlinear equations are linearized without losing the overall time accuracy. The Streamline Upwind Petrov-Galerkin method (SUPG) is applied for the weighted formulation of the Navier-Stokes equations. The combined method uses the three-node triangular element with equal-order interpolation functions for all the variables of the velocity components, the pressure and the temperature. Examples of the unsteady advection-diffusion problem in channel, the lid-driven cavity flow, and the thermally driven flow in concentric cylinder are selected to evaluate the performance of the presented method.

Keywords: Finite element method, Fractional step method, Unsteady incompressible flow

1. Introduction

Convection heat transfer is one of the most challenging problems for computational methods due to its inherent coupling between the governing equations of the fluid motion and the energy equation. This coupling effect can be seen noticeably at high Rayleigh numbers in free convection and forced convection problem. Another main reason which increases the difficulty for solving the convection heat transfer problems is due to the non-linear phenomenon of the convection terms presented in both the momentum equations and the energy equation. Several algorithms have been proposed and applied successfully to analyze these problems, such as the velocity-pressure segregated method [1-3] based on the SIMPLE algorithm and an unsteady algorithms based on the fractional step method [4, 5]. These two algorithms are similar in that they correct the velocity using the pressure derived from the continuity equation.

The objective of this paper is to develop a second-order time accurate numerical algorithm for analyzing unsteady incompressible Navier-Stokes equations. The algorithm uses the four-step fractional method with an equal-order triangular finite element and adopts the idea of the consistent SUPG [6, 7] as an upwind scheme. The time integration method is based on a fully implicit fractional step method and the resulting nonlinear momentum and energy equations are linearized without losing the overall time accuracy.

The paper starts from briefly describing the set of the partial differential equations that satisfy the law of conservation of mass, momentums and energy. Corresponding finite element equations are derived and the element matrices are presented. The computational procedure used in the development of the computer program is then described. Finally, the finite element formulation and the computer program are then verified by solving several examples that have exact solution and numerical solutions from other algorithms.

2. Theoretical formulation and solution procedure

2.1 Governing equations

The governing equations for the unsteady incompressible viscous flow consist of the conservation of mass which is the continuity equation, the conservation of momentums, and the conservation of energy, as follows,

Continuity equation,

$$\frac{\partial u_i}{\partial x_i} = 0 \tag{1a}$$

Momentum equations,

$$\frac{\partial u_i}{\partial t} + \frac{\partial}{\partial x_j}\left(u_i u_j\right) = -\frac{1}{\rho}\frac{\partial p}{\partial x_i} + \frac{\partial}{\partial x_j}\left(\nu \frac{\partial u_i}{\partial x_j}\right) - g_i\left(1-\beta\left(T-T_0\right)\right) \tag{1b}$$

Energy equation,

$$\frac{\partial T}{\partial t} + \frac{\partial}{\partial x_j}\left(u_j T\right) = \frac{\partial}{\partial x_j}\left(\tilde{k}\frac{\partial T}{\partial x_j}\right) + \tilde{Q} \tag{1c}$$

where i, j is 1, 2, x_j are the Cartesian coordinates, u_i are the corresponding velocity components, t is time, ρ is the density, p is the pressure, ν is the kinematic viscosity, g_i is the gravitational acceleration constant in the x and y direction, respectively, β is the volumetric coefficient of thermal expansion, T is the temperature, T_o is the reference temperature, $\tilde{k}$ is thermal diffusivity coefficient and $\tilde{Q}$ is the internal heat generation rate per unit volume.

2.2 Fractional four-step method

The governing differential equations are integrated in time using the fully implicit four-step fractional method [5]. The pressure gradient terms are first decoupled from those of the convection, diffusion and the external force terms. The second-order fully implicit time-advancement scheme of Crank-Nicolson is applied for both the convective and the viscous terms in Eqs. (1b-c). The pressure is then obtained from the continuity equation and the velocity is corrected by the pressure, as follows [8],

Step 1,
$$\frac{\hat{u}_i - u_i^n}{\Delta t} + \frac{1}{2}\frac{\partial}{\partial x_j}\left(\hat{u}_i \hat{u}_j + u_i^n u_j^n\right) = -\frac{1}{\rho}\frac{\partial p^n}{\partial x_i} + \frac{1}{2}\nu\frac{\partial}{\partial x_j}\left(\frac{\partial \hat{u}_i}{\partial x_j} + \frac{\partial u_i^n}{\partial x_j}\right) + g_i^n\left(1 - \beta\left(T^n - T_0\right)\right) \quad (2a)$$

Step 2,
$$\frac{u_i^* - \hat{u}_i}{\Delta t} = \frac{1}{2}\left(\frac{1}{\rho}\frac{\partial p^n}{\partial x_i}\right) \quad (2b)$$

Step 3,
$$\frac{\partial}{\partial x_i}\frac{\partial p^{n+1}}{\partial x_i} = \frac{2\rho}{\Delta t}\frac{\partial u_i^*}{\partial x_i} \quad (2c)$$

Step 4,
$$\frac{u_i^{n+1} - u_i^*}{\Delta t} = -\frac{1}{2}\left(\frac{1}{\rho}\frac{\partial p^{n+1}}{\partial x_i}\right) \quad (2d)$$

Step 5,
$$\frac{T^{n+1} - T^n}{\Delta t} + \frac{1}{2}\frac{\partial}{\partial x_j}\left(T^{n+1}u_j^{n+1} + T^n u_j^n\right) = \frac{1}{2}\tilde{k}\frac{\partial}{\partial x_j}\left(\frac{\partial T^{n+1}}{\partial x_j} + \frac{\partial T^n}{\partial x_j}\right) + \tilde{Q}^n \quad (2e)$$

where Δt is the time increment, $\hat{u}_i$ and u_i^* are the intermediate velocities, and superscript n denotes the time level. The time increment of the fully implicit method is restricted to achieve a desired solution accuracy, not by the numerical stability.

2.3 Finite element formulations

2.3.1 Streamline Upwind Petrov-Galerkin method

In the streamline upwind Petrov-Galerkin method, a modified weighting function, W_α, is applied to the convection terms for suppressing the non-physical spatial oscillation that may occur in the numerical solution. The weighting function is given by [7],

$$W_\alpha = N_\alpha + \frac{\Delta t_e}{2}u_j\frac{\partial N_\alpha}{\partial x_j} \quad (3)$$

when
$$\Delta t_e = \frac{\sigma h}{|U|} \quad (4a)$$

$$\sigma = \coth \mathrm{Pe} - \frac{1}{\mathrm{Pe}} \quad (4b)$$

$$\mathrm{Pe} = \frac{|U|h}{2\nu} \text{ and } |U| = \sqrt{u^2 + v^2} \quad (4c)$$

where Pe is the Peclet numbers and h is the minimum element size.

2.3.2 Discretization of the momentum and energy equations

The three-nodes triangular element is used in this study. The element assumes linear interpolation functions for the velocity components, the pressure, and the temperature as

$$\phi(x,y) = \sum_{\alpha=1}^{3} N_\alpha(x,y)\phi_\alpha \quad (5)$$

where ϕ denotes the transport property (u, v, p and T) and N_α are the element interpolation functions.

The method of weighted residuals with the streamline upwind Petrov-Galerkin method is employed to discretize the finite element equations by multiplying Eqs. (2a-e) by the weighting function. Integration by parts is then performed using the Gauss theorem to yield the element equations in the form,

Step 1,
$$\left(\frac{[M]}{\Delta t} + \frac{1}{2}\left([C] + [K_m]\right)\right)\{\hat{u}_i\} = \left(\frac{[M]}{\Delta t} - \frac{1}{2}\left([C] + [K_m]\right)\right)\{u\}^n - [G_i]\{p\}^n + \{R_{gi}\}^n + \{R_{bi}\}^n \quad (6a)$$

Step 2,
$$[M]\{u_i\}^* = [M]\{\hat{u}_i\} + \frac{\Delta t}{2}[G_i]\{p\}^n \quad (6b)$$

Step 3,
$$[K_p]\{p\}^{n+1} = \{R_u\}^* + \{R_v\}^* + \{R_b\}^* \quad (6c)$$

Step 4,
$$[M]\{u_i\}^{n+1} = [M]\{u_i\}^* - \frac{\Delta t}{2}[G_i]\{p\}^{n+1} \quad (6d)$$

Step 5,
$$\left(\frac{[M]}{\Delta t} + \frac{1}{2}\left([C] + [K_T]\right)\right)\{T\}^{n+1} = \left(\frac{[M]}{\Delta t} - \frac{1}{2}\left([C] + [K_T]\right)\right)\{T\}^n + \{R_c\}^n + \{R_q\}^n + \{R_Q\}^n \quad (6e)$$

In the above equations, the element matrices written in the integral form are,

$$[M] = \int_\Omega \{N\}\lfloor N \rfloor d\Omega \quad (7a)$$

$$[C] = \int_\Omega \{W\}\left(u_j\left\lfloor\frac{\partial N}{\partial x_j}\right\rfloor\right) d\Omega \quad (7b)$$

$$[K_m] = \nu\int_\Omega \left\{\frac{\partial W}{\partial x_j}\right\}\left\lfloor\frac{\partial N}{\partial x_j}\right\rfloor d\Omega \quad (7c)$$

$$[K_T] = \tilde{k}\int_\Omega \left\{\frac{\partial W}{\partial x_j}\right\}\left\lfloor\frac{\partial N}{\partial x_j}\right\rfloor d\Omega \quad (7d)$$

$$[G_i] = \frac{1}{\rho}\int_\Omega \{W\}\left\lfloor \frac{\partial N}{\partial x_i} \right\rfloor d\Omega \tag{7e}$$

$$[K_p] = \int_\Omega \left\{\frac{\partial W}{\partial x_j}\right\}\left\lfloor \frac{\partial N}{\partial x_j} \right\rfloor d\Omega \tag{7f}$$

$$\{R_g\} = g_i \int_\Omega \{W\}(\beta T - (1+\beta T_0))d\Omega \tag{7g}$$

$$\{R_u\} = \frac{2\rho}{\Delta t}\int_\Omega \left\{\frac{\partial W}{\partial x}\right\}\lfloor N \rfloor \{u\} d\Omega \tag{7h}$$

$$\{R_v\} = \frac{2\rho}{\Delta t}\int_\Omega \left\{\frac{\partial W}{\partial y}\right\}\lfloor N \rfloor \{v\} d\Omega \tag{7i}$$

$$\{R_{bi}\} = \nu \int_\Gamma \{W\}\left(\frac{\partial u_i}{\partial x_j}\hat{n}_k\right) d\Gamma \tag{7j}$$

$$\{R_b\} = -\frac{2\rho}{\Delta t}\int_\Gamma \{W\}(u_j \hat{n}_k)\, d\Gamma \tag{7k}$$

$$\{R_c\} = \tilde{k}\int_\Gamma \{W\}\left(\frac{\partial T}{\partial x_j}\hat{n}_k\right) d\Gamma \tag{7l}$$

$$\{R_q\} = \frac{1}{\rho c}\int_\Gamma \{W\} q_s \, d\Gamma \tag{7m}$$

$$\{R_Q\} = \frac{1}{\rho c}\int_\Omega \{W\} Q \, d\Omega \tag{7n}$$

where Ω is the element area and Γ is the element boundary. The local time step is assumed as the minimum between the convective local time step and diffusive local time step,

$$\Delta t = min(\Delta t_{conv}, \Delta t_{diff}) \tag{8}$$

$$\Delta t_{conv} = \frac{h}{|U|}, \quad \Delta t_{diff} = \frac{h^2}{2\tilde{k}} \tag{9}$$

where Re is the Reynolds number.

3. Results

Three example problems are presented to evaluate the proposed algorithm. The first and second examples, the unsteady advection-diffusion problem in channel and the lid-driven cavity flow, respectively, are chosen to evaluate the finite element formulation and to validate the developed computer program. The third example, the thermally driven flow in concentric cylinder, is used to evaluate the performance of the presented scheme for the analyzing the unsteady flow with fluid heat transfer.

3.1 Unsteady advection-diffusion problem in channel

The first example selected for evaluating the finite element formulation and validating the developed computer program is the unsteady advection-diffusion problem in channel [9]. The problem is described by a one-dimensional heat diffusion down a semi-infinite channel filled with a fluid that moves at a uniform velocity. The channel is 1.0 long and 0.1 wide. The entrance of the channel is kept at a constant temperature $T_1(0,t)$ of 100 for t > 0. The initial temperature of the channel $T_0(x,0)$ is 20 for $0 < x < 1$, while both sides of the channel are insulated. The fluid velocity is uniformly maintained at 0.5. The governing differential equation of this problem is given by,

$$\frac{\partial T}{\partial t} + u\frac{\partial T}{\partial x} = \tilde{k}\frac{\partial^2 T}{\partial x^2} \quad \text{for} \quad 0 < x < 1 \tag{10}$$

The exact solution of this problem is [8],

$$T(x,t) = T_0 + \frac{1}{2}(T_1 - T_0)\left[erfc\left(\frac{x-ut}{2\sqrt{\tilde{k}t}}\right) + e^{ux/\tilde{k}}\, erfc\left(\frac{x+ut}{2\sqrt{\tilde{k}t}}\right)\right] \tag{11}$$

Figure 1 shows the comparison of the numerical results with the exact solutions at different times. The figure shows good agreement of the predicted and the exact solutions.

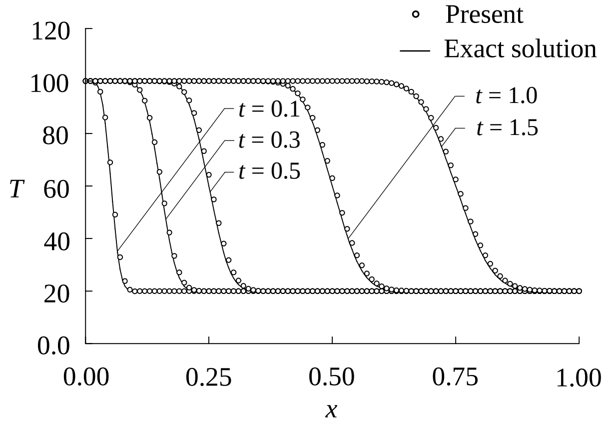

Figure 1. Comparative solutions of the unsteady advection diffusion problem in channel for $\tilde{k} = 0.001$

3.2 The lid-driven cavity flow

The lid-driven cavity flow is one of the examples commonly selected for evaluating new numerical algorithms for analyzing viscous incompressible flow. The square cavity has no-slip condition along the bottom and the side walls, while the top-lid moves to the right at the horizontal velocity of one as shown in Fig. 2. The finite element model used in the presented analysis consisting of 2,601 nodes and 5,000 elements is also shown in the figure.

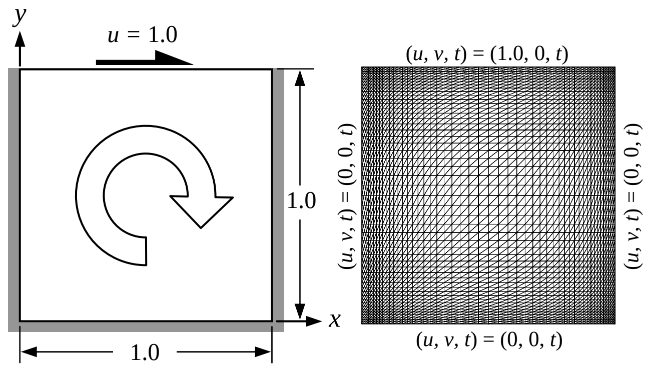

Figure 2. Problem statement and finite element model of the lid-driven cavity flow problem.

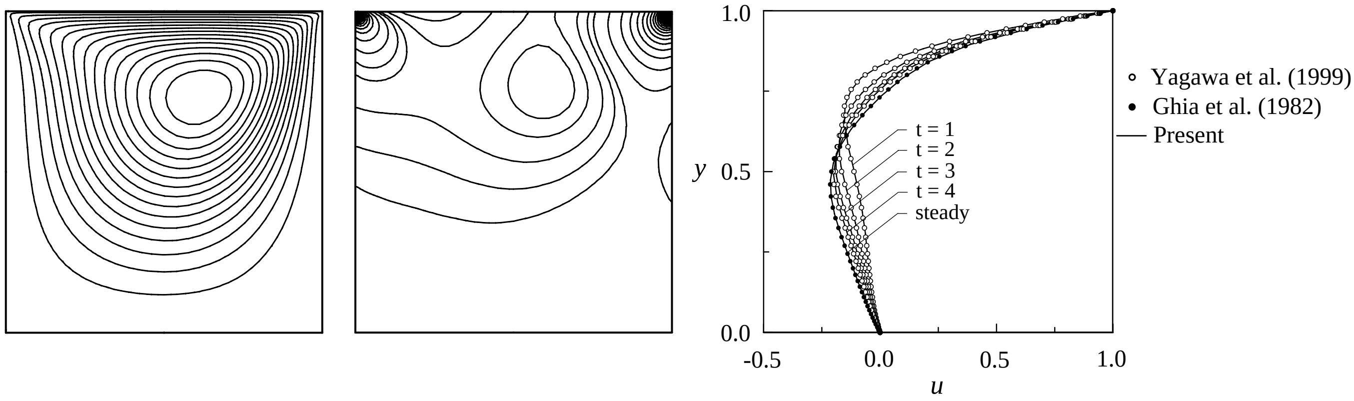

Figure 3. Predicted streamline, pressure contours and velocity profile of *x*-direction on *x* = 0.5 at Re = 100.

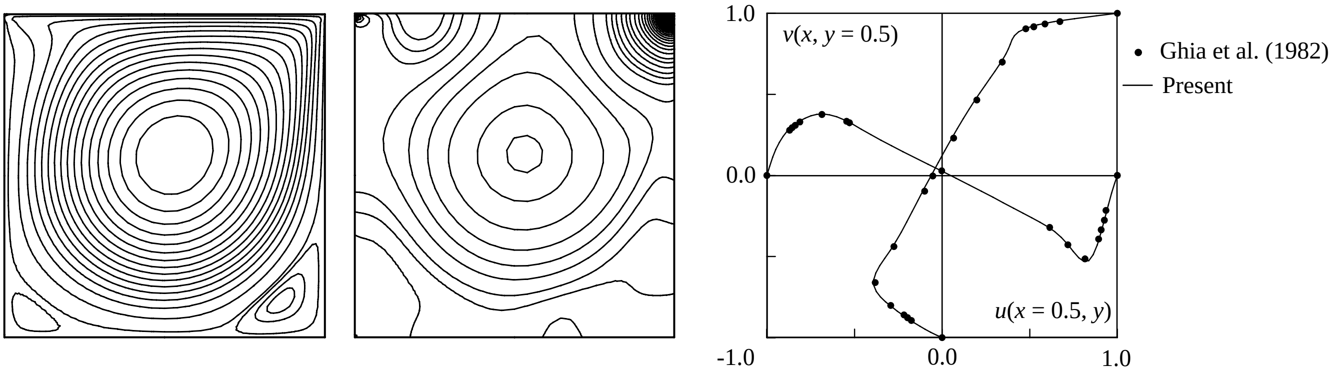

(a) Re = 1,000

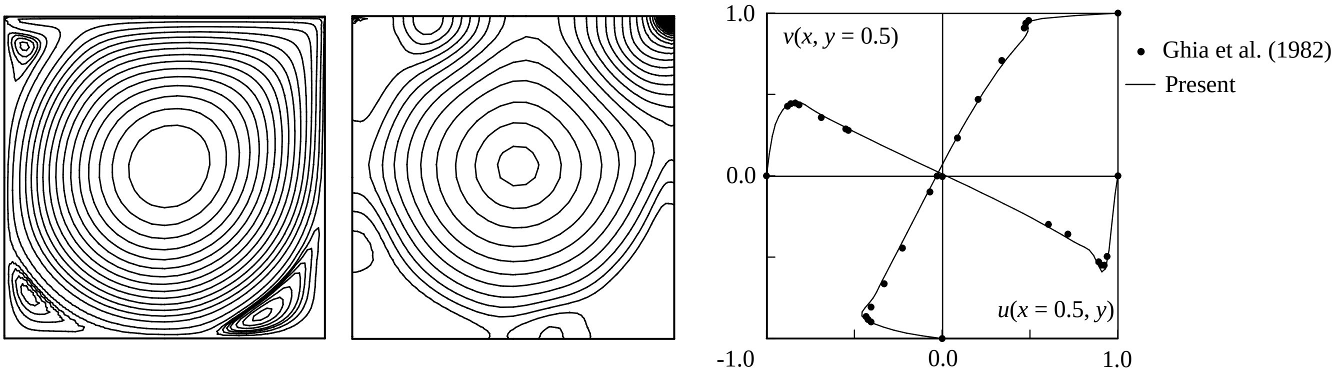

(b) Re = 5,000

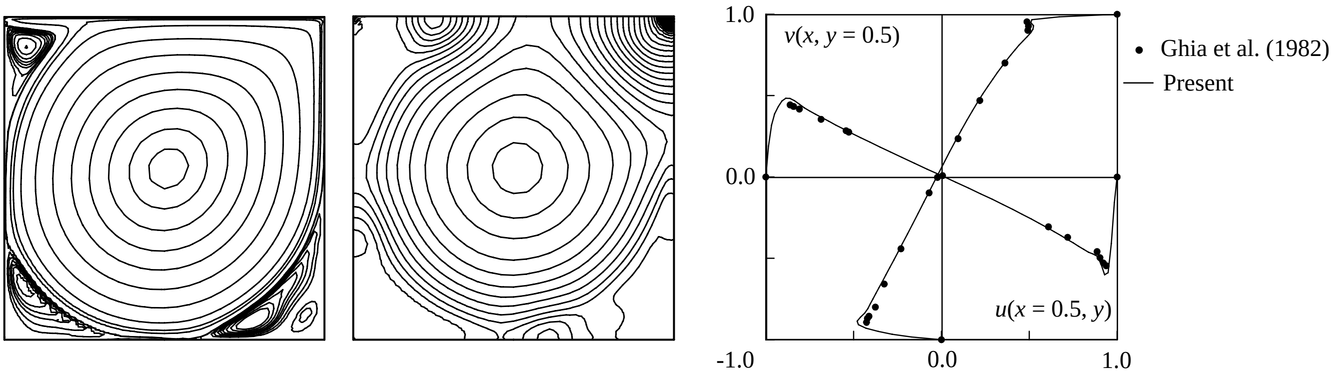

(c) Re = 10,000

Figure 4. Predicted streamline, pressure contours and velocity profiles in the *x* and *y* directions at Re = 1,000, 5,000 and 10,000.

Figure 3 shows the predicted streamline, pressure contours and the comparative solutions of the *u*-velocity profiles at the time of 1, 2, 3, 4, all for the Reynolds of 100. The results are compared with those presented by Yagawa et al. [10], and the steady-state solution of Ghia et al. [11]. The left figure shows the relatively smooth streamline contours of the flow that circulates in the clockwise direction. Figure 4 shows the predicted steady-state solutions as compared to those presented in Ref. [11] for the Reynolds numbers of 1,000, 5,000 and 10,000, respectively. These figures highlight good agreement between the predicted and the solutions obtained from other existing algorithms.

3.3 Thermally driven flow in concentric cylinders

The thermally driven flow in concentric cylinders, as shown in Fig. 5, is selected to evaluate the performance of the presented algorithm for the problem with a more complex geometry. The fluid is freely convected in the annular space between long, horizontal concentric cylinders due to high temperature on the inner cylinder and lower temperature on the outer cylinder. This problem was studied experimentally by Kuehn and Goldstein [12] for which their results can be used for comparison. All results are at the Prandtl number of 0.7 with a ratio of gap width to inner-cylinder diameter (L/D) of 0.8. The finite element model consisting of 2,170 nodes and 4,200 elements are shown in Fig. 6. Figure 7 presents the predicted temperature contours on the left half and the velocity vectors on the right half at the Rayleigh numbers of 3,000 and 10,000. Figure 8 shows the comparisons of the equivalent conductivities at the inner and outer cylinder surfaces. The figures show good agreement of the predicted solutions and the experimental results.

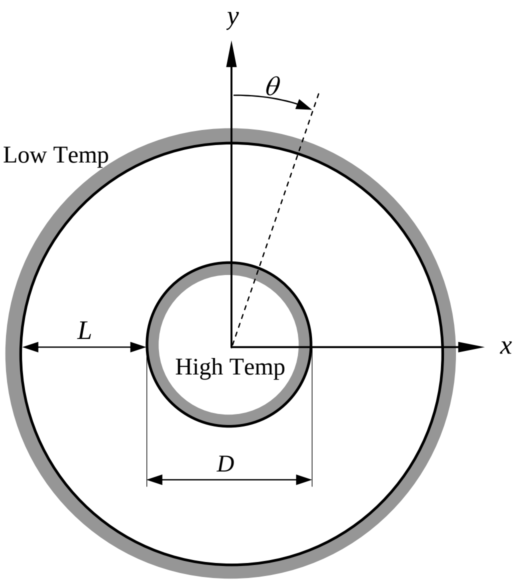

Figure 5. Thermally driven flow in concentric cylinders.

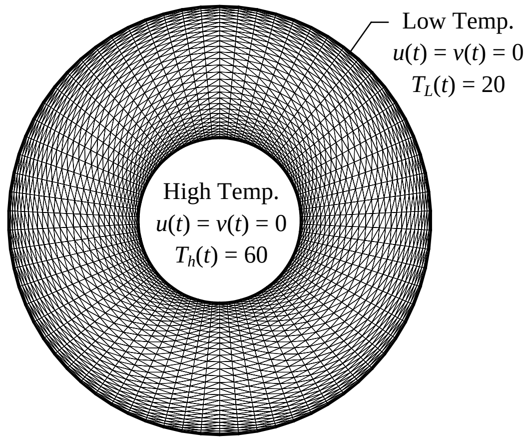

Figure 6. Finite element model for thermally driven flow in concentric cylinders.

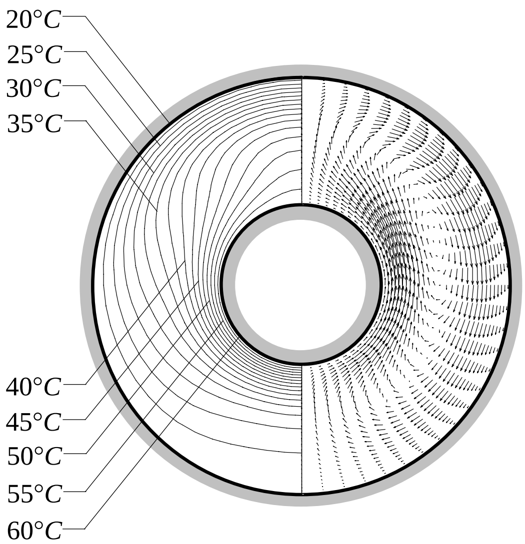

(a) Ra = 3,000

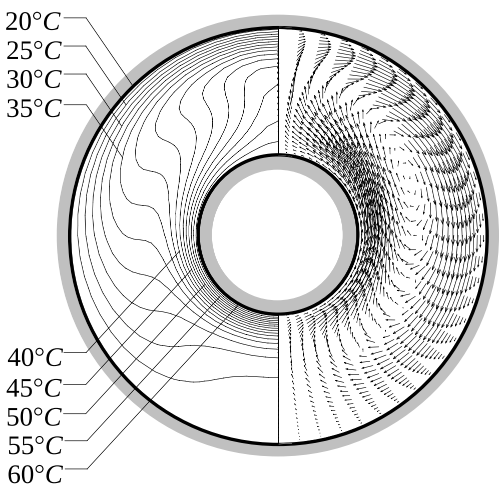

(b) Ra = 10,000

Figure 7. Predicted temperature contours and velocity vectors at Rayleigh numbers of 3,000 and 10,000.

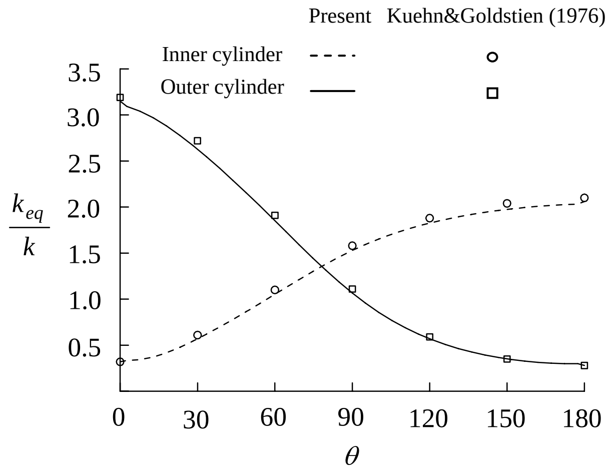

(a) Ra = 3,000

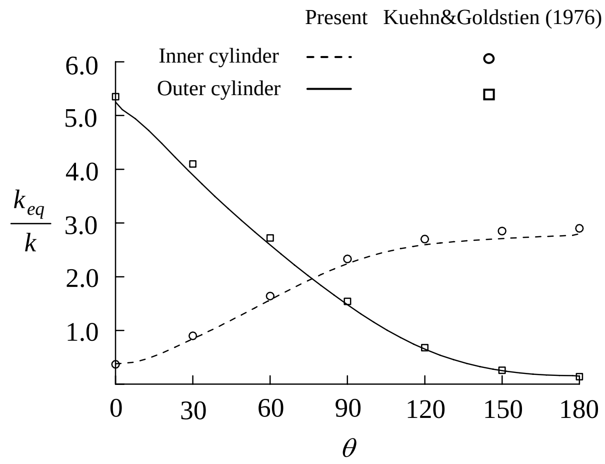

(b) Ra = 10,000

Figure 8. Comparison of the local equivalent conductivities at Rayleigh numbers of 3,000 and 10,000.

4. Conclusion

A second-order time accurate finite element algorithm with a fully implicit fractional four-step method for analysis of the unsteady incompressible flow with heat transfer was presented. The consistent SUPG method was adopted and applied on the convection terms to suppress any non-physical spatial oscillation that might occur in the numerical solution. The proposed algorithm used a segregated solution procedure to compute the velocities, the pressure and the temperature separately to improve the computational efficiency. All the finite element equations were derived and a corresponding computer program was developed. The performance of the proposed finite element algorithm was evaluated by comparing its predicted solutions with those obtained from other existing algorithms.

Acknowledgments

The authors are pleased to acknowledge the Thailand Research Fund (TRF) for supporting this research work.

References

[1] Rice, J.G. and Schnipke, R.J., 1986. An equal-order velocity-pressure formulation that does not exhibit spurious pressure modes. Computer Methods in Applied Mechanics and Engineering, Vol.58, pp. 135-149.

[2] Choi, H.G. and Yoo, J.Y., 1995. A hybrid numerical method for Navier-Stokes equations based on SIMPLE algorithm. Numerical Heat Transfer Part B, Vol.28, pp. 155-170.

[3] Wansophark, N. and Dechaumphai, P., 2004. Combined adaptive meshing technique and segregated finite element algorithm for analysis of free and forced convection heat transfer. Finite Elements in Analysis and Design, Vol.40, pp. 645-663.

[4] Ramaswamy, B. and Jue, T.C., 1992. Some recent trends and developments in finite element analysis for incompressible thermal flow. International Journal Numerical Methods Engineering, Vol.35, pp. 671-707.

[5] Choi, H.G. et al., 1997. A fractional four-step finite element formulation of the unsteady incompressible Navier-Stokes equations using SUPG and linear equal-order element methods. Computer Methods in Applied Mechanics and Engineering, Vol.143, pp. 333-348.

[6] Brooks, A.N. and Hughes, T.J.R., 1982. Streamline Upwind/Petrov-Galerkin Formulations for Convection Dominated Flows with Particular Emphasis on the Incompressible Navier-Stokes Equations. Computer Methods in Applied Mechanics and Engineering, Vol.32, pp. 199-259.

[7] Zienkiewicz, O.C. and Taylor, R.L., 2000. The Finite Element Method, 5th ed, McGraw-Hill, Oxford, Butterworth-Heinemann.

[8] Ferziger, J.H. and Peric, M., 1999. Computational Methods for Fluid Dynamics. Tokyo, Springer.

[9] Kythe, P.K. and Wei, D., 2004. An Introduction to Linear and Nonlinear Finite Element Analysis, Birkhauser, Boston, Berlin.

[10] Yagawa, G., and Shirazaki, M., 1999. Parallel Computing for Incompressible Flow using a Nodal-Based Method. Computational Mechanics, Vol. 23, pp. 209-217.

[11] Ghia, U., Ghia, K.N., and Shin, C.T., 1982. Hight-Re Solutions for Incompressible Flow Using the Navier-Stokes Equations and a Multigrid Method. Journal of Computational Physics, Vol. 48, pp. 387-411.

[12] Kuehn, T.H., and Goldstein, R.J., 1976. An Experimental and Theoretical Study of Natural Convection in the Annulus between Horizontal Concentric Cylinders. Journal of Fluid Mechanic, Vol. 74, pp. 695-719.